Erythrosin Isothiocyanate Selectively Labels Lysine$_{464}$ within an ATP-Protectable Binding Site on the Ca-ATPase in Skeletal Sarcoplasmic Reticulum Membranes†

Shaohui Huang, Sewite Negash, and Thomas C. Squier*

Department of Biochemistry, Cell and Molecular Biology, University of Kansas, Lawrence, Kansas 66045-2106

Received February 3, 1998; Revised Manuscript Received March 23, 1998

ABSTRACT: Conditions that permit the selective modification of an ATP-protectable site on the Ca-ATPase in skeletal sarcoplasmic reticulum (SR) membranes using erythrosin isothiocyanate (Er-ITC) have been identified. The major labeling site for Er-ITC has been identified using reversed-phase HPLC and positive FAB mass spectrometry after exhaustive tryptic digestion of the Er-ITC-modified Ca-ATPase. An ATP-protectable peptide corresponding to M_{452}NVFNTEVRNLSK$_{464}$VER$_{467}$ is modified by Er-ITC, the average mass of which is 2830.1 ± 0.3 Da. The exclusive modification of lysine residues indicates Lys$_{464}$ as the site of Er-ITC modification. Derivatization with Er-ITC diminishes the secondary activation of steady-state ATPase activity and the rate of dephosphorylation by millimolar concentrations of ATP. In contrast, in the presence of micromolar ATP concentrations Er-ITC modification of the Ca-ATPase does not affect (i) the apparent affinity of ATP, (ii) the maximal extent of phosphoenzyme formation by ATP, (iii) the rate of steady-state ATP hydrolysis, or (iv) the rate of dephosphorylation of the Ca-ATPase. Furthermore, ATP utilization by the Ca-ATPase is unaffected by detergent solubilization, irrespective of Er-ITC modification, indicating that the secondary activation of ATP hydrolysis involves a single Ca-ATPase polypeptide chain. Therefore, Er-ITC does not interfere with the normal structural transitions associated with phosphoenzyme decay. Rather, these results indicate that Er-ITC bound to Lys$_{464}$ interferes with either ATP binding to a low-affinity site or the associated structural transitions that modulate the rate of enzyme dephosphorylation.

The Ca-ATPase[1] present in sarcoplasmic reticulum (SR) membranes functions to resequester calcium ions following excitation−contraction coupling, mediating the rate-limiting step of muscle contraction in both skeletal and cardiac muscle (*1*). The transport mechanism of the Ca-ATPase requires the structural linkage between the formation of an acyl phosphate at Asp$_{351}$ and the spatially distant high-affinity calcium binding sites located within the transmembrane helices (*2*). Two classes of nucleotide-binding sites have been resolved under equilibrium conditions using fluorescent analogues of ATP (*3*, *4*). On the basis of these and other results, it has been suggested that more than one ATP binds to each Ca-ATPase polypeptide chain at physiologically relevant ATP concentrations (*4*, *5*). ATP bound in the high-affinity class of nucleotide site(s) is the substrate for phosphoenzyme formation (*6*). In contrast, occupancy of the low-affinity class of nucleotide-binding site(s) by ATP does not alter the level of phosphoenzyme formation but rather enhances the rate of phosphoenzyme hydrolysis and calcium transport (*7*−*10*). The secondary activation of the Ca-ATPase by millimolar concentrations of ATP may provide a regulatory mechanism to modulate the catalytic activity of the Ca-ATPase. However, the mechanism involving the secondary activation of the Ca-ATPase by millimolar concentrations of ATP remains uncertain and has been suggested to involve (i) differences in the nucleotide affinity within a single catalytic ATP binding cleft that arises during the enzymatic cycle, (ii) the presence of multiple ATP binding sites located within a single Ca-ATPase polypeptide chain, or (iii) alternating conformational states involving structurally coupled nucleotide-binding sites located on neighboring Ca-ATPase polypeptide chains (*5*, *11*−*14*). In the present study we have used erythrosin isothiocyanate (Er-ITC) to derivatize a site on the Ca-ATPase that blocks the secondary activation of ATP hydrolysis and dephosphorylation by millimolar concentrations of ATP, without affecting either the apparent nucleotide affinity or rates of ATP hydrolysis and dephosphorylation in the presence of micromolar concentrations of ATP. The relative affinities and catalytic activities associated with the high- and low-affinity nucleotide requirements for catalytic activity were found to be independent of oligomeric interactions between Ca-

† Supported by NIH Grant GM46837. The tandem mass spectrometer was purchased with the aid of NIH Grant S10 RR0 6294 and by the University of Kansas.

* Author to whom correspondence should be addressed. Telephone: (785) 864-4008. Fax: (785) 864-5321. E-mail: tcsquier@kuhub.cc.ukans.edu.

[1] Abbreviations: ADP, adenosine 5′-diphosphate; ATP, adenosine 5′-triphosphate; BSA, bovine serum albumin; Ca-ATPase, Ca^{2+}- and Mg^{2+}-dependent ATPase; $C_{12}E_8$, polyoxyethylene 8 lauryl ether; DET, dithioerythritol; DMF, *N*,*N*-dimethylformamide; DTT, dithiothretiol; EGTA, ethylene glycol bis(β-aminoethyl ether)-*N*,*N*,*N*′,*N*′-tetraacetic acid; Er-ITC, erythrosin 5-isothiocyanate; ESI, electrospray ionization; FAB, fast atom bombardment; FITC, fluoroscein isothiocyanate; FRET, fluorescence resonance energy transfer; HPLC, high-performance liquid chromatography; MOPS, 3-(*N*-morpholino)propanesulfonic acid; MS, mass spectrometry; NADH, reduced form of α-nicotinamide adenine dinucleotide; PEP, phospho(enol)pyruvate; SDS−PAGE, sodium dodecyl sulfate−polyacrylamide gel electrophoresis; SR, sarcoplasmic reticulum; TEMED, *N*,*N*,*N*′,*N*′-tetramethylethylenediamine; TPCK, L-(tosylamido-2-phenyl) ether chloromethyl ketone; Tris, tris(hydroxymethyl)aminomethane; VP, 4-vinylpyridine.

S0006-2960(98)00275-X CCC: $15.00
Published on Web 04/23/1998

ATPase polypeptide chains, indicating that the secondary activation of ATPase activity by millimolar concentrations of ATP is a manifestation of the catalytic activity of a single Ca-ATPase polypeptide chain. To identify the amino acid(s) modified by Er-ITC, the Er-ITC-labeled Ca-ATPase was proteolytically digested, an ATP-protectable Er-ITC modified peptide was separated by reversed-phase HPLC, and the Er-ITC-labeled peptide was identified using positive FAB mass spectrometry.

EXPERIMENTAL PROCEDURES

Materials. Dithiothreitol (DTT) and KCl were purchased from Research Organics Inc. (Cleveland, OH). Acrylamide, bisacrylamide, TEMED, and ammonium persulfate were purchased from Bio-Rad (Richmond, CA). Sucrose, NaCl, ammonium bicarbonate, acetonitrile, Tris (free base), and MOPS were purchased from Fisher Scientific (Pittsburgh, PA). $CaCl_2$ standard solutions were purchased from VWR (St. Louis, MO). Er-ITC (isomer II), FITC (isomer I), ATP (vanadate free disodium salt), ADP (potassium salt), NADH (disodium salt), TPCK-treated trypsin (type III), 4-vinylpyridine (VP), A23187, EGTA, $MgCl_2$, and HPLC grade ammonium acetate were purchased from Sigma (St. Louis, MO). Er-ITC (isomer I) was purchased from Molecular Probes Inc. (Junction City, OR). PEP (monopotassium salt) was purchased from Boehringer (Indianapolis, IN). Bovine serum albumin (BSA) was purchased from Pierce (Rockford, IL). Polyoxyethylene 8 lauryl ether ($C_{12}E_8$) was purchased from Nikkol Chemical Co. (Tokyo, Japan). Pyruvate kinase and lactate dehydrogenase were purchased from Worthington (Freehold, NJ). SR membranes were isolated from rabbit fast-twitch skeletal muscle, essentially as previously described (*15*), and were stored in 20 mM MOPS (pH 7.0) and 0.3 M sucrose (sucrose buffer) at −70 °C.

Enzymatic Activity Assays. The calcium-dependent ATPase activity was measured either as an ammonium molybdate complex of phosphate (*16*) or using an enzyme-linked assay as previously described (*17*). Measurements of total and calcium-independent ATPase activity involved the addition of the indicated concentration of an equimolar solution of $MgCl_2$ and ATP to 0.02 mg/mL of SR vesicles in a medium containing 35 mM MOPS (pH 7.0), 100 mM KCl, 5 mM $MgCl_2$, 4 μM A23187, and either 100 μM $CaCl_2$ or 2 mM EGTA at 25 °C. Measurements made using the enzyme-linked assay included 0.15 mM NADH, 2 mM PEP, 10 units of pyruvate kinase activity, and 32 units of lactate dehydrogenase activity. In the latter case, the rate of ATP regeneration was determined by the direct addition of ADP and in all cases was >3 times faster than ATP hydrolysis rates. Maximal levels of phosphoenzyme formation from ATP and rates of dephosphorylation were measured as previously described (*9*, *18*, *19*).

Chemical Derivatization with FITC or Er-ITC. The chemical modification of the Ca-ATPase with either FITC or Er-ITC was carried out in the dark, essentially as previously described (*21*, *22*). Briefly, SR membranes (2 mg/mL) were incubated with variable concentrations of either FITC or Er-ITC in 30 mM Tris (pH 8.7), 5 mM $MgCl_2$, and 100 mM KCl (labeling buffer) for 15 min at 25 °C. Samples were immediately diluted at least 5-fold with ice-cold buffer A [i.e., 30 mM MOPS (pH 7.0), 0.3 M sucrose, and 1 mg/mL BSA] and were incubated on ice for 45 min. SR membranes were then pelleted by centrifugation at 100000*g* for 45 min, resuspended in sucrose buffer [20 mM MOPS (pH 7.0) and 0.3 M sucrose], centrifuged again, and finally resuspended in sucrose buffer. To assess whether Er-ITC modified an ATP-protectable site, 20 mM ATP was added to the labeling buffer, as described under Results. SR protein concentration was determined according to the Biuret method, using BSA as a standard (*23*). Quantitation of the Er-ITC and FITC labeling stoichiometries involved the measurement of the absorbance spectrum following solubilization of labeled SR samples in 1% SDS and 0.1 N NaOH, using the following measured extinction coefficients: ϵ_{536}(Er-ITC) = 87 800 M^{-1} cm^{-1} and ϵ_{491}(FITC) = 71 700 M^{-1} cm^{-1}. Since the covalent labeling of the Ca-ATPase with either Er-ITC or FITC was found to interfere with the determination of the protein concentration using the Biuret assay, the absorbance at 280 nm associated with aromatic amino acids in SR proteins corrected for the absorbance (*A*) associated with either Er-ITC or FITC bound to the Ca-ATPase was used to determine the protein concentration (mg/mL) in these cases, where ϵ_{280nm}(SR) = 1.15 mg^{-1} cm^2, ϵ_{280}(Er-ITC) = 24 100 M^{-1} cm^{-1}, and ϵ_{280}(FITC) = 23 500 M^{-1} cm^{-1}, using the following formula for either Er-ITC- or FITC-modified SR membranes:

$$[\text{SR protein}] = [A^{SR}_{280nm} - (A^{Er-ITC}_{536nm}\epsilon^{Er-ITC}_{280nm}/\epsilon^{Er-ITC}_{536nm})]/\epsilon^{SR}_{280nm}$$

or

$$[A^{SR}_{280nm} - (A^{FITC}_{491nm}\epsilon^{FITC}_{280nm}/\epsilon^{FITC}_{491nm})]/\epsilon^{SR}_{280nm}$$

Visualization of Fluorescently Labeled Proteins. FITC- and Er-ITC-modified proteins were separated using SDS−PAGE, essentially as described previously (*24*). Protein bands were stained with Coomassie Brilliant Blue G. Alternatively, the fluorescence associated with FITC- and Er-ITC-labeled proteins were visualized after either a Schott OG515 or a RG540 long-pass filter using an MP4 camera (Polaroid Corp., Cambridge, MA) to detect the fluorescence associated with individual protein bands.

Tryptic Digestion. Prior to tryptic digestion, SR membranes (2 mg/mL) were incubated in 100 mM NH_4HCO_3 (pH 8.0), 2 mM DTT, and 100 μM $CaCl_2$ at 50 °C for 15 min to reduce disulfide bonds. Exhaustive tryptic digestion of the cytoplasmic portion of the Ca-ATPase involved the addition of TPCK-treated trypsin (0.04 mg/mL) to SR vesicles at 37 °C for 4 h. Soluble peptides were separated from the SR membranes by centrifugation at 100000*g* for 30 min. Thiol groups on the tryptic peptides (0.2 mg/mL) were alkylated with 10 mM VP for 1.5 h prior to lyophilization to prevent the formation of disulfide cross-links between tryptic peptides. Proteolytic fragments were dissolved in 10 mM ammonium acetate (pH 6.5) prior to reversed-phase HPLC separation (see below).

Reversed-Phase HPLC Separation of Tryptic Peptides. The separation of proteolytic fragments obtained from the cytoplasmic portion of the Ca-ATPase was carried out using an ISCO HPLC instrument (Lincoln, NE), composed of a model 2360 gradient programmer, a model 2350 pump, a V^4 variable wavelength absorbance detector, and a Phenomenex (Torrance, CA) C_4 reversed-phase column employing a linear gradient varying from 10 mM ammonium acetate (pH 6.5) to 10 mM ammonium acetate (pH 6.5) and 30%

(v/v) acetonitrile in water at a rate of 0.45% per minute, essentially as described previously (*25*). The peptide elution profiles were respectively monitored using either 214 nm to assess the extent of tryptic cleavage or 536 nm to detect tryptic peptides derivatized with Er-ITC. The detected peaks were collected manually and were pooled, lyophilized, and subjected to fast atom bombardment (FAB) mass spectrometry (see below). Mass identification was assisted through the use of software (GPMAW from Lighthouse Data, Odense, Denmark) that permits the identification of all possible combinations associated with the cDNA-derived amino acid sequence of the SERCA1 isoform of the Ca-ATPase resulting from proteolytic digestion of the Ca-ATPase that are consistent with an observed experimental mass (*26*).

Mass Spectrometry Experiments. Mass spectra were obtained using an Autospec-Q tandem hybrid mass spectrometer (VG Analytical Ltd., Manchester, U.K.). FAB positive mass spectrometry experiments were performed using a cesium gun operated at 20 keV energy and 2 μA emission, essentially as previously described (*27*). Peptides dissolved in 50% CH_3CN (v/v) were added to an identical volume of DTT and DET (4:1) as a matrix. Electrospray ionization (ESI) spectra were acquired using the Autospec-Q equipped with a VG Mark IV ESI source (Micromass Ltd., Manchester, U.K.). This instrument has the "pepper pot" counter electrode and hexapole transfer optics. The instrument was operated in positive ion mode at 4 kV acceleration potential, ESI needle at 7.5 kV, and counter electrode at 5 kV. Remaining lenses were optimized for maximum sensitivity using a solution containing 500 fmol/μL lysozyme (Sigma) dissolved in a solution containing 70% (v/v) methanol and 0.5% (v/v) acetic acid. The instrument was tuned to 1800 resolving power and scanned from 500 to 3000 Da at 10 s per decade. Mass calibration was done with a CsI solution. Tryptic peptides were dissolved in 70% (v/v) methanol and were infused into the ESI source at 8 μL/min through a 130 μm i.d. stainless steel needle and nebulized with a coaxial gas flow of nitrogen at 10 L/h.

Fluorescence Measurements. Steady-state polarization measurements were obtained on an ISS (Champaign, IL) K2 frequency domain fluorometer, as previously described (*28*). Measurements involved 0.05 mg/mL of the FITC-derivatized Ca-ATPase in 35 mM MOPS (pH 7.0), 0.1 M KCl, 5 mM $MgCl_2$, 100 μM $CaCl_2$, and 0.3 M sucrose at 25 °C. FITC was excited using the 493 nm line obtained from an argon ion laser (Coherent, Palo Alto, CA), and the resulting fluorescence signal was detected after a Schott OG530 longpass filter.

RESULTS

Er-ITC Preferentially Labels Sites on the Ca-ATPase in Native SR Membranes. To determine the labeling specificity of Er-ITC, we have examined the protein-associated fluorescence after separation of labeled and unlabeled SR proteins by SDS−PAGE. In agreement with earlier observations (*22*, *29*−*31*), we find that irrespective of whether the Ca-ATPase is labeled with a low or high molar stoichiometry, the fluorescence signals associated with both Er-ITC and FITC co-localize exclusively with the Ca-ATPase (data not shown). No other SR proteins are labeled with either FITC or Er-ITC to any appreciable extent. Thus, under these labeling conditions Er-ITC selectively labels sites on the Ca-ATPase in native SR membranes.

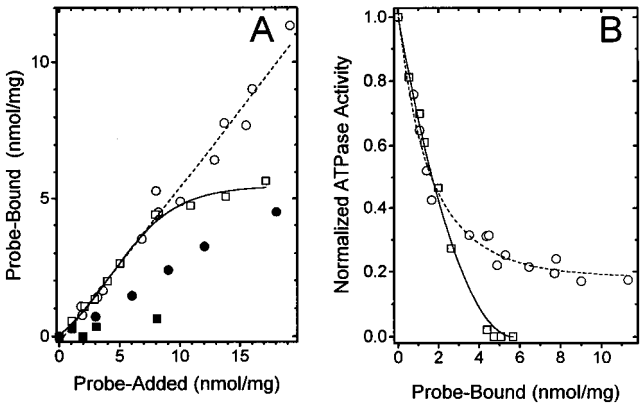

FIGURE 1: Binding and inactivation profiles associated with Er-ITC or FITC modification of Ca-ATPase: extent of labeling (A) and inhibition of ATPase activity (B) associated with variable amounts of added Er-ITC (○, ●) or FITC (□, ■) in the absence (○, □) or presence (●, ■) of 20 mM ATP during labeling. Labeling conditions involved 2 mg/mL SR protein in 0.1 M KCl, 5 mM $MgCl_2$, and 30 mM Tris (pH 8.7), as described under Experimental Procedures.

*Selective Labeling of an ATP-Protectable Site within the Ca-ATPase by Er-ITC. W*e have characterized the relationship between the stoichiometry of Er-ITC labeling and the resulting inactivation of the Ca-ATPase, comparing it with that of FITC. FITC has previously been shown to block binding of nucleotides but not of smaller phosphoryl compounds such as acetyl phosphate or carbamoyl phosphate (*10*). In the case of Er-ITC, we find that at low labeling stoichiometries its reactivity is virtually identical to that of FITC and that, like FITC, the presence of ATP during the labeling reaction decreases the incorporation of Er-ITC (Figure 1A), suggesting that Er-ITC *may* label sites within or near the nucleotide-binding pocket. However, while FITC modification of the Ca-ATPase, which is specific for Lys_{515}, saturates at a stoichiometric ratio of 1 mol of FITC/mol of Ca-ATPase polypeptide chains (i.e., 5.3 ± 0.1 nmol of FITC/mg of SR protein), Er-ITC modification of the Ca-ATPase does not saturate at stoichiometric ratios. Furthermore, ATP is less effective in blocking Er-ITC incorporation (Figure 1A), suggesting that Er-ITC labels additional sites outside the nucleotide-binding cleft.

The incorporation of FITC results in the inactivation of Ca-ATPase catalytic activity (Figure 1B), which is consistent with previous kinetic data suggesting that FITC and ATP compete for overlapping binding sites (*21*). Whereas incorporation of one FITC per Ca-ATPase polypeptide chain results in complete inhibition of enzymatic activity, a similar extent of Er-ITC incorporation results in the retention of 20−25% of the initial calcium-dependent ATPase activity (Figure 1B). The residual ATPase activity observed at high labeling stoichiometries suggests that while Er-ITC modification greatly reduces the catalytic activity, the Ca-ATPase retains the ability to hydrolyze ATP. Furthermore, the ability to label additional sites on the Ca-ATPase with Er-ITC with no further inhibition of ATPase activity indicates that the incorporation of Er-ITC on some sites results in little inhibition of ATPase activity. Differences in labeling specificity between FITC and Er-ITC are not the result of

differences involving the reactive isothiocyanate moiety, since one observes virtually identical inactivation profiles using two different isomers of Er-ITC with the isothiocyanate group at position 2′ (isomer I) or 3′ (isomer II) in the carboxybenzyl ring.

The similar inhibition of ATP hydrolysis associated with low stoichiometries of either Er-ITC or FITC suggests that Er-ITC also preferentially modifies sites that interfere with ATP binding or utilization. The effect of Er-ITC modification on ATP binding in the catalytic site was measured from the maximal level of phosphoenzyme formed from [γ-^{32}P]-ATP. We find that the maximal level of phosphoenzyme formed in native SR is 4.6 ± 0.2 nmol/mg. Upon incorporation of 1.0 nmol of Er-ITC/mg of SR (where Er-ITC incorporation is most selective), there is essentially no decrease in the extent of phosphoenzyme formation (4.3 ± 0.2 nmol/mg), indicating that low levels of Er-ITC modification do not inhibit ATP binding within the catalytic site. Thus, the inhibition of steady-state ATPase activity associated with Er-ITC incorporation (Figure 1) is probably related to the inhibition of phosphoenzyme hydrolysis, which is rate-limiting under conditions of saturating ATP (*32*). In contrast, modification of the Ca-ATPase with FITC blocks ATP binding and the formation of phosphoenzyme (*21*). These results suggest that FITC and Er-ITC label different sites.

Er-ITC Interferes with the Secondary Enzymatic Activation by Millimolar Concentrations of ATP. The effect of Er-ITC labeling on the ATP dependence of Ca-ATPase activity is shown in Figure 2. In agreement with previous results, we observe a biphasic relationship between calcium-dependent ATPase activity in native SR membranes and ATP concentration (*7*, *34*, *35*), indicating that the catalytic activity of the Ca-ATPase has a high- and low-affinity nucleotide requirement, with apparent affinities in the micromolar and millimolar range, respectively. Incorporation of Er-ITC into the Ca-ATPase results in selective inhibition of the catalytic activity associated with the low-affinity nucleotide requirement (Figure 2; Table 1). On the other hand, the apparent affinity and rate of ATP hydrolysis associated with the high-affinity nucleotide requirement are essentially unaffected by the incorporation of Er-ITC. Extrapolation of the inhibition associated with the low-affinity nucleotide requirement suggests that the incorporation of 4.3 ± 1.2 nmol of Er-ITC/mg of SR protein (i.e., 1 mol of Er-ITC/mol of Ca-ATPase) results in the complete inhibition of the secondary activation of ATPase activity by millimolar concentrations of ATP (see inset in Figure 2). The selective inhibition of the secondary activation of ATPase activity by Er-ITC, with no corresponding alteration in the levels of phosphoenzyme formation, suggests that Er-ITC modifies a site that interferes with either binding of ATP to a low-affinity site or the associated structural coupling within the catalytic site normally associated with substrate utilization.

Solubilizing Concentrations of $C_{12}E_8$ Stabilize the Monomeric Form of the Ca-ATPase. To investigate the possible structural coupling between the nucleotide-binding domains of neighboring Ca-ATPase polypeptide chains, conditions were first defined that ensure complete disruption of interactions between Ca-ATPase polypeptide chains present in native SR membranes, without displacing protein-associated phospholipids (PALs) necessary to stabilize the monomeric Ca-ATPase polypeptide chain in a native conformation (*36*−*39*). Therefore, to monitor detergent-induced disruption of protein−protein associations, we have taken advantage of the sensitivity of steady-state polarization measurements to fluorescence resonance energy transfer (FRET) between FITC bound to Lys_{515} between neighboring Ca-ATPase polypeptide chains (*40*). For example, increased FITC incorporation results in a progressive decrease in the steady-state polarization (Figure 3A), reflecting increased FRET as FITC labeling sites are saturated. Upon subsequent addition of solubilizing concentrations of detergent to SR samples containing variable amounts of bound FITC (see below), the observed steady-state polarization is independent of labeling stoichiometry as a result of the abolition of FRET. Thus, the decrease in polarization observed when the amount of

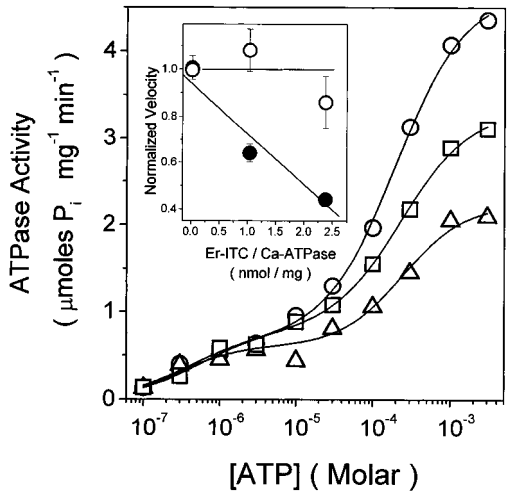

FIGURE 2: Effect of Er-ITC on the biphasic ATP-dependent activation of the Ca-ATPase in native SR membranes: calcium-dependent ATPase activity associated with the Ca-ATPase in native SR (○) and after the incorporation of 1.0 (□) or 2.4 nmol/mg (△) Er-ITC. ATPase activity was measured with an enzyme-linked assay described under Experimental Procedures. Data were fit using the method of nonlinear least squares to the following equation: $V_{total} = V_{max_1}[\text{Mg-ATP}]^n/(K_{M_1} + [\text{Mg-ATP}]^n) + V_{max_2}[\text{Mg-ATP}]^n/(K_{M_2} + [\text{Mg-ATP}]^n)$, as previously described (*36*). In this equation, V_{total} is the observed ATPase activity, V_{max_1} and V_{max_2} are the respective maximal catalytic rate constants, and K_{M_1} and K_{M_2} are the apparent dissociation constants associated with the high- and low-affinity nucleotide requirements for catalytic activity. The Hill coefficient (n) accounts for possible cooperativity between high- and low-affinity classes of nucleotide-binding sites. In all cases $n = 1$, indicating independent binding of ATP to high- and low-affinity nucleotide-binding sites. (Inset) The maximal velocity associated with the high-affinity (V_{max_1}, ○) and low-affinity (V_{max_2}, ●) classes of nucleotide-binding site(s) as a function of the incorporation of Er-ITC, normalized to the activities corresponding to native SR (i.e., $V_{max_1} = 0.71 \pm 0.06$ μmol of P_i mg^{-1} min^{-1}; $V_{max_2} = 3.9 \pm 0.2$ μmol of P_i mg^{-1} min^{-1}). Errors were propagated (*55*).

Table 1: Kinetic Constants Associated with ATP-Dependent Activation of the Ca-ATPase in Native SR[a]

	high-affinity site		low-affinity site	
sample (nmol of Er-ITC/mg)	K_{m1} (μM)	V_{max1} (μmol mg^{-1} min^{-1})	K_{m2} (mM)	V_{max2} (μmol mg^{-1} min^{-1})
native SR	0.4 ± 0.1	0.71 ± 0.06	0.19 ± 0.03	3.9 ± 0.2
1.0 nmol/mg	0.5 ± 0.1	0.77 ± 0.05	0.22 ± 0.03	2.5 ± 0.1
2.4 nmol/mg	0.3 ± 0.1	0.61 ± 0.06	0.27 ± 0.08	1.7 ± 0.1

[a] Ca-ATPase activity was measured and analyzed as described in the legend in Figure 2, where K_m and V_{max} are the apparent dissociation constants and maximal catalytic rate constants associated with the high- and low-affinity nucleotide binding sites.

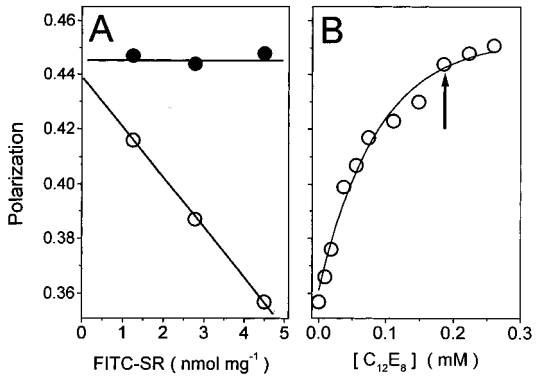

FIGURE 3: Disruption of oligomeric interactions between Ca-ATPase polypeptide chains by detergent solubilization. Alterations in steady-state polarization associated with FITC covalently bound to Lys_{515} on the Ca-ATPase permit the detection of interactions between individual Ca-ATPase polypeptide chains for native SR (○) or after detergent solubilization upon the addition of 0.2 mM $C_{12}E_8$ (●) (A) and the determination of the necessary amount of detergent to disrupt these interactions (B). The arrow in panel B indicates the concentration of $C_{12}E_8$ used to solubilize SR membranes in panel A. Experimental conditions include 0.05 mg/mL FITC-labeled SR membranes in 35 mM MOPS (pH 7.0), 100 μM $CaCl_2$, 5 mM $MgCl_2$, 0.1 M KCl, and 0.3 M sucrose. The temperature was 25 °C. Conditions associated with the fluorescence polarization measurements are described under Experimental Procedures.

FITC incorporation is increased arises from FRET between neighboring Ca-ATPase polypeptide chains, and after detergent solubilization the Ca-ATPase is a monomer.

The minimal amount of $C_{12}E_8$ necessary to disrupt interactions between Ca-ATPase polypeptide chains was determined from the influence of added $C_{12}E_8$ on the steady-state polarization associated with an SR sample fully modified with FITC (i.e., 4.5 nmol of FITC/mg) (Figure 3B). There is a progressive enhancement of the steady-state polarization associated with FITC (Figure 3B), and at 200 μM $C_{12}E_8$ the steady-state polarization approaches a limiting value ($P \approx 0.45$) that is near that associated with FITC bound to the Ca-ATPase in native SR extrapolated to low labeling stoichiometries where there is no FRET (Figure 3A). Under these conditions essentially all of the Ca-ATPase is solubilized, as indicated by the inability to sediment significant amounts of SR membranes (100000g_{max} for 45 min). The solubilizing concentration of $C_{12}E_8$ used in these experiments (200 μM) is unlikely to displace the PALs, since 7 mM $C_{12}E_8$ has previously been shown to be required to displace PALs (*38*). In agreement, the Ca-ATPase is functionally stable for hours under these solubilizing conditions.

Biphasic ATP-Dependent Activation of Individual Ca-ATPase Polypeptide Chains. The solubilization of the Ca-ATPase using $C_{12}E_8$ results in only a minimal decrease in the maximal calcium-dependent ATPase activity relative to that observed in native SR membranes (Figure 4), consistent with earlier suggestions that interactions between Ca-ATPase polypeptide chains are not essential to the catalytic activity of the Ca-ATPase (*37*). Significantly, there is a secondary activation of calcium-dependent ATPase activity in the presence of submillimolar ATP concentrations of the monomeric form of the Ca-ATPase that is analogous to that observed for the Ca-ATPase in native SR membranes (Figure 4). Detergent solubilization has a minimal effect on the apparent affinities of either the high- or low-affinity nucleotide requirements for catalytic activity for both native SR and after Er-ITC modification (Tables 1 and 2). Extrapolation of the inhibition associated with the low-affinity nucleotide requirement indicates that incorporation of 4.3 ± 0.3 nmol of Er-ITC/mg of SR protein results in complete inhibition of the secondary activation of ATPase activity by millimolar concentrations of ATP (see inset in Figure 4). These latter results are in agreement with the stoichiometries of Er-ITC associated with the inhibition of the secondary activation of ATPase activity in native SR (i.e., 4.3 ± 1.2 nmol of Er-ITC/mg of SR protein). Thus, Er-ITC modification selectively inhibits the secondary activation of ATPase activity by millimolar ATP concentrations, irrespective of the presence of oligomeric interactions between Ca-ATPase polypeptide chains (see inset in Figures 2 and 4; Tables 1 and 2). These results indicate that both the high- and low-affinity nucleotide requirements are a manifestation of the catalytic activity of a single Ca-ATPase polypeptide chain.

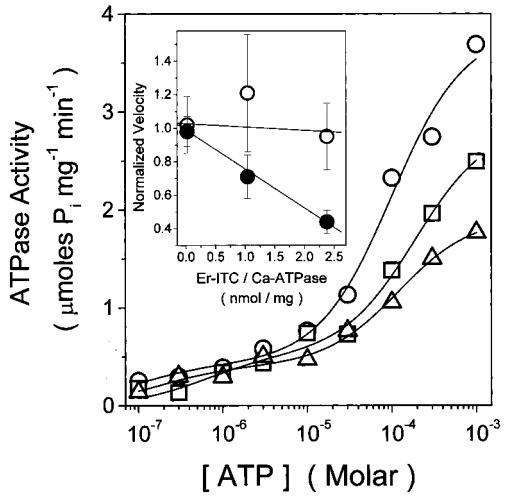

FIGURE 4: ATP-dependent activation of detergent solubilized Ca-ATPase at variable Er-ITC labeling stoichiometries. Calcium-dependent ATPase measurements following the addition of 0.2 mM $C_{12}E_8$ associated with the unlabeled Ca-ATPase (○) and after the covalent incorporation of 1.0 (●) or 2.4 nmol/mg (△) of Er-ITC were measured using the enzyme-linked assay, as described under Experimental Procedures. (Inset) Normalized maximal velocities associated with the high-affinity (V_{max_1}, ○) and low-affinity (V_{max_2}, ●) nucleotide requirements for catalytic activity as a function of Er-ITC incorporation. Both the experimental conditions and data analysis were as described in the legend to Figure 2.

Table 2: Kinetic Constants Associated with ATP-Dependent Activation of the Detergent-Solubilized Ca-ATPase[a]

	high-affinity site		low-affinity site	
sample (nmol of Er-ITC/mg)	K_m (μM)	V_{max} (μmol mg^{-1} min^{-1})	K_m (mM)	V_{max} (μmol mg^{-1} min^{-1})
native SR	0.2 ± 0.1	0.42 ± 0.07	0.10 ± 0.02	3.4 ± 0.3
1.0 nmol/mg	0.6 ± 0.4	0.51 ± 0.12	0.19 ± 0.10	2.4 ± 0.4
2.4 nmol/mg	0.2 ± 0.1	0.40 ± 0.05	0.12 ± 0.04	1.5 ± 0.2

[a] Ca-ATPase activity was measured and analyzed as described in the legend in Figure 2, where K_m and V_{max} are the apparent dissociation constants and maximal catalytic rate constants associated with the high- and low-affinity nucleotide binding sites.

Rates of Phosphoenzyme Decomposition. To distinguish between alterations in the nucleotide-binding cleft that result from Er-ITC modification of Lys_{464} that may modulate the binding affinity of ATP during the catalytic cycle of the Ca-ATPase from alterations in the rate of phosphoenzyme

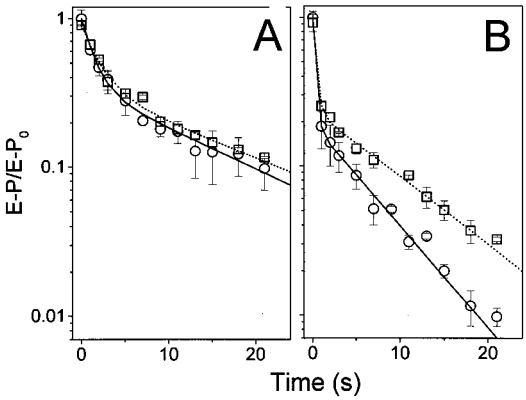

FIGURE 5: ATP-dependent activation of phosphoenzyme decomposition. Rates of dephosphorylation were measured for native SR (○) and after the incorporation of 1.2 nmol/mg$^-$ of Er-ITC (□) in the presence of either 1 μM (A) or 5 mM (B) ATP. Phosphoenzyme was formed by the incubation of SR vesicles with 1 μM [γ-^{32}P]-ATP in reaction buffer [35 mM MOPS (pH 7.0), 0.1 M KCl, 5 mM $MgCl_2$, 0.1 mM $CaCl_2$, and 3 μM A23187] for 5 s. Time-dependent decay of phosphoenzyme was measured after a 20-fold dilution of the phosphorylated Ca-ATPase into dilution buffer containing either 1 μM ATP (A) or 5 mM ATP (B), and at the indicated times the reaction was quenched in 1 N TCA and 10 mM NaH_2PO_4. SR vesicles were retained on a 0.45 μm nitrocellulose filter for scintillation counting, as previously described (*19*). Data were fit using the method of nonlinear least squares to the following rate equation: $E-P/E-P_0 = A_1e^{-k_1t} + A_2e^{-k_2t}$, where $E-P$ corresponds to the observed level of phosphoenzyme, $E-P_0$ represents the initial level of phosphoenzyme, and k_1 and k_2 represent rate constants associated with the fast and slow phases of phosphoenzyme decay, respectively. Maximal levels of phosphoenzyme were 4.6 ± 0.2 and 4.4 ± 0.2 nmol/mg of SR protein for the native and Er-ITC-modified Ca-ATPase. All reactions were performed at 0 °C. Error bars represent the standard deviation of two separate measurements.

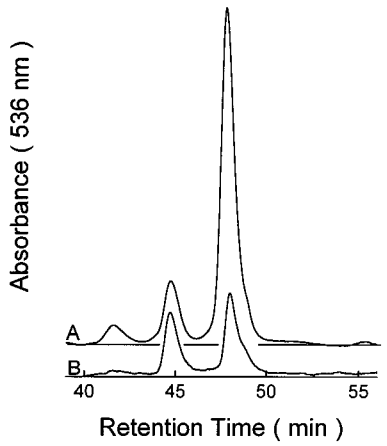

FIGURE 6: Reversed-phase HPLC separation of tryptic peptides that are modified with Er-ITC. Two representative chromatograms are shown corresponding to resolved Er-ITC-modified peptides detected at 536 nm after exhaustive tryptic digestion (4 h, 37 °C) and separation of the cytoplasmic peptides of the Ca-ATPase labeled in the presence of 4.0 μM Er-ITC in the absence (A) and presence (B) of 20 mM ATP, which result in the respective incorporation of 1.0 and 0.37 nmol of Er-ITC/mg of SR protein. The maximal absorbance associated with the major peak in the top chromatogram is 0.04 M^{-1} cm^{-1}.

hydrolysis, we have measured the rate of dephosphorylation of native and Er-ITC-modified Ca-ATPase. As already described, the extent of Er-ITC modification was chosen to minimize nonspecific labeling (see above) and corresponds to 1.2 and 2.8 nmol of Er-ITC/mg of SR protein. In native SR that rate of dephosphorylation is biphasic (Figure 5), reflecting conformational transitions associated with the interconversion between the ADP-sensitive and -insensitive forms of the Ca-ATPase that accompany calcium occlusion (*19*, *20*). In the absence of saturating nucleotide concentrations, Er-ITC modification of Lys_{464} does not modify the rates of phosphoenzyme hydrolysis (Figure 5A; Table 3), indicating that Er-ITC does not alter the conformational transitions involving either the formation of the ADP-insensitive phosphoenzyme or the subsequent steps involving phosphoenzyme hydrolysis. In contrast, the enhanced rate of dephosphorylation associated with native (unmodified) Ca-ATPase observed in the presence of saturating concentrations of ATP is diminished by Er-ITC (Figure 5B). Thus, Er-ITC either interferes with ATP binding to a low-affinity site or alters conformational changes involving the nucleotide-binding cleft that are normally associated with phosphoenzyme hydrolysis upon nucleotide association with a low-affinity site.

Table 3: Phosphoenzyme Decay Rate Constants of the Ca-ATPase[a]

	sample[a]					
			Er-ITC- labeled Ca-ATPase			
	control		1.2 nmol/mg		2.8 nmol/mg	
[ATP] (μM)	k_1 (s^{-1})	k_2 (s^{-1})	k_1 (s^{-1})	k_2 (s^{-1})	k_1 (s^{-1})	k_2 (s^{-1})
1.0	0.7 (0.1)	0.06 (0.01)	0.5 (0.1)	0.06(0.01)	0.7 (0.1)	0.06 (0.01)
10.0	1.2 (0.1)	0.08 (0.01)	0.8 (0.3)	0.09 (0.01)	1.1 (0.2)	0.06 (0.01)
5000	3.5 (0.1)	0.16 (0.01)	2.9 (0.4)	0.11 (0.01)	1.5 (0.4)	0.08 (0.01)

[a] Rates of phosphoenzyme hydrolysis were measured and analyzed as described in the legend in Figure 5, where k_1 and k_2 are the apparent rates of phosphoenzyme hydrolysis. Standard deviations of the measured values are indicated in parentheses.

Reversed-Phase HPLC Separation and Mass Spectrometric Identification of an ATP-Protectable Peptide Covalently Modified with Er-ITC. The ability of Er-ITC to selectively interfere with the low-affinity nucleotide requirement associated with the secondary activation of the catalytic activity of the Ca-ATPase offers the possibility of identifying this site within the primary sequence of the Ca-ATPase. The primary labeling site associated with Er-ITC was identified after exhaustive digestion with trypsin of the Er-ITC-modified Ca-ATPase using reversed-phase HPLC and FAB-mass spectrometry, as described under Experimental Procedures. These experiments utilized low labeling stoichiometries (i.e., 1.0 nmol of Er-ITC/mg of SR protein), where the inactivation data suggest that the specificity of Er-ITC incorporation into an ATP-protectable binding site is most specific (Figure 1). Following proteolytic digestion and centrifugation of the membrane vesicles, 91 ± 3% of the bound Er-ITC was released into the supernatant; these peptides were separated using reversed-phase HPLC, and 76 peptide fragments were resolved (data not shown), in good agreement with previous results (*41*). Using the associated absorbance of Er-ITC at 536 nm to detect labeled peptides, three peaks with retention times of 42, 45, and 48 min were resolved (Figure 6). The peak at 48 min accounts for 81% of the labeled peptides and is diminished by the presence of ATP during the labeling reaction, suggesting that this peak contains a peptide that has been modified with Er-ITC at an ATP-protectable site. Using FAB-mass spectrometry to identify the multiple peptides contained within the major elution peak, we resolve the masses of seven different

Table 4: Identification of Er-ITC-Modified Peptide by FAB-MS[a]

$[M + H^+]_{exptl}$[b]	$[M + H^+]_{theor}$[c]	peptide sequence
713.2	713.4	$D_{568}TPPKR_{573}$
1154.6	1156.6	$K_{481}EFTLEFSR_{489}$[d]
1339.7	1337.7	$D_{557}TLRC^eLALATR_{567}$[d]
1517.0	1516.9	$A_{219}LGIVATTGVSTEIGK_{234}$
1839.9	1839.1	$S_{335}LPSVETLGCTSVICSDK_{352}$
2178.3	2178.5	$D_{144}IVPGDIVEVAVGDKVPADIR_{164}$
2830.1	2830.2	$M_{452}NVFNTEVRNLS\mathbf{K_{464}}VER_{467}$[f]

[a] Correspondence between resolved experimental masses and proposed peptide sequences generated after tryptic digestion of the Ca-ATPase, as described under Experimental Procedures. [b] Monoisotopic masses are resolved for peptides with masses <1800 Da, while average masses are reported for peptides with larger molecular masses. Experimental errors associated with FAB-MS measurements are <1 Da. [c] Theoretical monoisotopic and average masses of peptides corresponding to expected tryptic fragments calculated from the amino acid sequence, as described under Experimental Procedures. [d] Peptides with experimental masses 1154.6 and 1339.7 are tentatively identified due to the significant mass difference from that predicted from the amino acid sequence. However, since Er-ITC modification blocks tryptic cleavage at adjacent sites, these low-mass peptides can be excluded as Er-ITC labeling sites due to the small size of Er-ITC-labeled peptides with correspondingly small molecular masses, which would contain at most two and four amino acids, respectively. [e] Cysteine modified with vinyl pyridine, whose respective monoisotopic mass is 105.06 Da. [f] Contains Er-ITC, the average molecular mass of which is 893.0 Da.

peptides that vary in molecular mass from 713 to 2830 Da (Table 4). Since Er-ITC derivatization of the Ca-ATPase is specific for lysine residues under these experimental conditions, it is possible to assign the resolved masses to tryptic peptides released from the Ca-ATPase. A consideration of all possible cytoplasmic peptides generated after the proteolytic cleavage of the Ca-ATPase by trypsin (where Er-ITC modification of lysine blocks the proteolytic cleavage by trypsin) suggests that there should be no Er-ITC-labeled peptides with molecular masses >3692 Da. Therefore, since FAB-MS can resolve peptides with masses <4000 (*27*), it is expected that the FAB-MS spectrum resolves all Er-ITC-labeled peptides.

The majority of the peptides resolved by FAB-MS are not labeled with Er-ITC (Table 4). However, there is one peptide with a resolved molecular mass of 2830.1 Da that corresponds to an Er-ITC-labeled peptide with the sequence M_{452}-$NVFNTEVRNLSK_{464}VER_{467}$, the theoretical molecular mass of which is 2830.2 Da. While R_{460} is not cleaved by trypsin in these experiments, in a complementary experiment involving the separation and identification of peptides derivatized with Er-ITC, we observed a peptide with a molecular mass of 1737.2 Da that corresponds to the Er-ITC-derivatized mass of the peptide with the sequence $N_{461}LSK_{464}VER_{467}$. Complementary electrospray mass spectrometry experiments were used to resolve possible additional labeled peptides that were not observed using FAB-MS as a result of their higher masses. We find no evidence that any additional peptides are labeled with Er-ITC. These results indicate that K_{464} is the primary labeling site for Er-ITC.

DISCUSSION

Er-ITC has been used in a number of time-resolved transient absorption and phosphorescence anisotropy measurements that have investigated structural alterations of the Ca-ATPase that may be important to the transport mechanism (*22*). However, the identity of chemically modified sites on the Ca-ATPase and their functional consequences have not been determined. Therefore, we have compared the labeling and inactivation profiles associated with Er-ITC modification of the Ca-ATPase with that of FITC, which is structurally homologous to Er-ITC and selectively labels Lys_{515} and prevents ATP binding to the Ca-ATPase. Following exhaustive tryptic digestion of the Ca-ATPase, we have isolated Er-ITC-modified peptides using reversed-phase HPLC chromatography and positive FAB-MS to identify the major labeling site of Er-ITC on the Ca-ATPase. The loss of the secondary activation of ATPase activity and phosphoenzyme hydrolysis by millimolar concentrations of ATP upon Er-ITC derivitization indicates that Er-ITC either blocks occupancy of the low-affinity class of ATP binding sites or disrupts the structural coupling between a low-affinity ATP binding site and the phosphoanhydride involving Asp_{351} in the catalytic site.

Relationship between Sites Modified by Er-ITC and FITC. Both Er-ITC and FITC react specifically with the Ca-ATPase at ATP-protectable sites within the cytoplasmic domain, as evidenced by (i) the correspondence of the fluorescence associated exclusively with the Ca-ATPase band on SDS−PAGE gels, (ii) the ability of both probes to be quantitatively released from the native SR membrane following exhaustive tryptic digestion, (iii) the loss of ATPase activity accompanying chemical modification of the Ca-ATPase, and (iv) the ability of ATP to block probe incorporation (Figure 1A). However, while FITC specifically labels Lys_{515} and prevents ATP from binding and phosphoenzyme formation (*21*, *30*), we find that Er-ITC selectively modifies Lys_{464} and blocks the secondary activation of ATPase activity and phosphoenzyme decomposition by millimolar concentrations of ATP without affecting either the maximal extent of phosphoenzyme formation or the rates of ATP hydrolysis and dephosphorylation at micromolar concentrations of ATP (Figures 2 and 5; Tables 1 and 3).

High- and Low-Affinity Nucleotide Requirements of the Ca-ATPase. In the presence of millimolar concentrations of ATP, the enzymatic activity of the Ca-ATPase increases relative to that observed in the presence of micromolar concentrations of ATP (Figure 2). Since there is no corresponding increase in phosphoenzyme formation (*8*), these results have been interpreted in terms of a regulatory function for a low-affinity nucleotide-binding site. Several possible explanations have been suggested for this secondary activation of the Ca-ATPase by millimolar concentrations of ATP including (a) subunit interactions between an oligomeric complex involving multiple Ca-ATPase polypeptide chains (*8*, *32*, *36*), (b) the presence of multiple nucleotide-binding sites on a single Ca-ATPase polypeptide chain (*14*), or (c) a kinetic effect involving the occupancy of a single catalytic binding site by ATP prior to phosphoenzyme hydrolysis (*6*, *12*).

The possible role of allosteric interactions between nucleotide-binding sites on adjacent Ca-ATPase polypeptide chains has been controversial. From the loss of the secondary activation of Ca-ATPase activity by solubilizing concentrations of detergent, the importance of regulatory interactions involving neighboring Ca-ATPase polypeptide chains has been suggested (*36*). However, this loss of secondary activation in detergent solubilized preparations may instead be related to the removal of PALs by the high concentrations

of detergents used to solubilize the Ca-ATPase, since PALs are known to be essential for optimal Ca-ATPase activity (*37*, *38*, *42*). To explore this possibility, we have used FRET between FITC-labeled preparations of the Ca-ATPase to determine the minimal amount of detergent necessary to disrupt interactions between Ca-ATPase polypeptide chains without the loss of PALs (Figure 3B). The similar biphasic ATP-dependent activity of the Ca-ATPase in native SR membranes and following the disruption of oligomeric interactions by detergent solubilization provides strong evidence that the secondary activation of the Ca-ATPase is unrelated to possible structural interactions between Ca-ATPase polypeptide chains (Figures 2 and 4; Tables 1 and 2). Furthermore, phosphoenzyme levels of native and detergent solubilized preparations are nearly identical (*9*), indicating that the reported incomplete phosphorylation of the catalytic sites in native SR membranes (*33*) is not related to interactions between Ca-ATPase polypeptide chains. These results further indicate that the biphasic ATP-dependent activation of the Ca-ATPase arises as a result of the catalytic activity of a single Ca-ATPase polypeptide chain.

However, it has remained controversial whether there are two independent ATP binding sites or if the nucleotide affinity of a single binding site is modulated by structural differences involving, for example, phosphoenzyme formation (*12*, *43*, *44*). The observation of multiple classes of ATP binding sites with differing affinities that can be kinetically resolved and the ability of nonhydrolyzable analogues of ATP (e.g., AMPPCP) to promote the activation of ATPase activity together suggest that there may be multiple nucleotide-binding sites associated with each individual Ca-ATPase polypeptide chain (*3*, *7*, *12*, *45*). In contrast, other measurements suggest that only a single nucleotide can bind to each Ca-ATPase polypeptide chain (*6*, *46*). These differences arise, in part, as a result of problems associated with the accurate determination of the absolute stoichiometries of Ca-ATPase polypeptide chains in an SR preparation (*9*, *33*). We find that Er-ITC modification of Lys_{464} selectively blocks the secondary activation of both ATP hydrolysis and phosphoenzyme decomposition by millimolar concentrations of ATP without altering the apparent binding affinity of the high-affinity nucleotide requirement of the Ca-ATPase (Figures 2 and 5; Table 1). Since Er-ITC incorporation does not interfere with the conformational transitions involving phosphoenzyme hydrolysis at low ATP concentrations (Table 3), it is unlikely that Er-ITC interferes with the long-range conformational transitions intrinsic to the conformational coupling between the phosphoanhydride at Asp_{351} and the high-affinity calcium binding sites located in the transmembrane sequences. Rather, these results suggest that Er-ITC interferes with either ATP binding to a low-affinity site or associated structural changes that modulate the rate of phosphoenzyme hydrolysis upon low-affinity ATP binding.

Relationship between Er-ITC Labeling Site on Lys_{464} and Other Residues Located within the Nucleotide-Binding Cleft. It is of interest to consider the proximity of Lys_{464} with respect to other sites that have been identified within the nucleotide-binding cleft. A model summarizing the relationship between sites of chemical modification within the nucleotide-binding cleft has been proposed by Green and co-workers (*47*, *48*). The majority of the sites that affect nucleotide binding and utilization are located within the cytoplasmic portion of the Ca-ATPase between S4 and S5, which represent the stalk sequences connecting the cytoplasmic domains of the Ca-ATPase to the transmembrane sequences M4 and M5. The major labeling site of Er-ITC at Lys_{464} is found to be proximal within the primary sequence of the Ca-ATPase to other sites of chemical modification that have been proposed to be associated with the nucleotide-binding cleft, including fluorescein maleimide (C_{471}), 2′, 3′-O-(2,4,6-trinitrophenyl)-8-azido-AMP (K_{492}), FITC (K_{515}), 8-azidoadenosine 5′-diphosphate (T_{532} and T_{533}), and adenosine triphosphopyridoxyl (K_{684}) (*21*, *41*, *47*, *49*, *50*). The clustering of the ATP-protectable labeling sites involving Er-ITC, FITC, and fluorescein maleimide (FMal) supports other measurements that suggest that erythrosin and fluorescein compete for a single ATP-protectable binding site on the Ca-ATPase (*14*). It should be noted that differences in the specificity of Er-ITC and FITC with respect to the sites of modification within the Ca-ATPase are expected, since previous results suggest that differences involving the reactive moiety and chromophoric group can result in differences in the pattern of chemical modification (*41*). Furthermore, the large steady-state polarization associated with FITC bound to the Ca-ATPase at low stoichiometries (where there is no FRET) indicates that bound FITC is strongly immobilized within a cleft (Figure 3A), suggesting that the bulkier Er-ITC may not fit within the fluorescein binding pocket.

Possible Sequences Associated with the Secondary Activation of the Ca-ATPase by Millimolar ATP Concentrations. It has previously been demonstrated that the large cytoplasmic sequence of the Ca-ATPase folds into an autonomous structure having the ability to bind nucleotide with high affinity (*5*, *51*). On the basis of the sequence homology with nucleotide-binding domains of water soluble kinases, it has been suggested that the primary sequence of the Ca-ATPase located between sequences S4 and S5 is folded into two distinct domains associated with high-affinity ATP binding and phosphoenzyme formation, respectively, that are conformationally coupled through a hinge region (*52*). In particular, sequences between Lys_{492} and S5 in the Ca-ATPase, highly conserved among all P-type ATPases, have been suggested to comprise the high-affinity nucleotide binding site on the basis of experiments showing both mutationally sensitive residues that alter ATPase activity and the covalent cross-linking of a range of different nucleotide analogues to amino acids within this sequence. In contrast, amino acids located toward the amino terminus of this cytoplasmic sequence are less highly conserved among different P-type ATPases, and the modification of Glu_{439}, Lys_{464}, and Cys_{471} within this sequence by bulky chromophoric moieties does not alter ATP binding, phosphoenzyme formation, or the rates of ATP hydrolysis (*41*, *53*, *54*), indicating that chemical modification of these residues does not interfere with ATP binding or substrate utilization. Rather, the disruption of the secondary activation of both ATPase activity and phosphoenzyme decay normally observed in the presence of millimolar concentrations of ATP without altering the utilization of ATP or the rate of dephosphorylation in the presence of micromolar concentrations of ATP suggests that this sequence may be important to either low-affinity ATP binding or structural transitions

normally involved in the enzyme reaction mechanism.

Conclusions and Future Directions. The disruption of the secondary ATP-dependent activation of ATP hydrolysis and phosphoenzyme hydrolysis by Er-ITC modification of Lys_{464} within the cytosolic domain of the Ca-ATPase has important functional implications with respect to the regulation of the enzymatic activity of the Ca-ATPase. Since Er-ITC modification of Lys_{464} does not alter either the maximal extent of phosphoenzyme formation or the rates of ATP hydrolysis and dephosphorylation in the presence of micromolar concentrations of ATP, it is unlikely that Er-ITC interferes with structural changes normally associated with the transport mechanism of the Ca-ATPase. Rather, Er-ITC interferes with either ATP binding or the structural coupling between a low-affinity ATP-binding site and the phosphoanhydride at Asp_{351}. Future time-resolved spectroscopic measurements should take advantage of these specific labeling conditions for the attachment of Er-ITC to Lys_{464} to probe dynamic structural changes within the cytoplasmic domain that are relevant to the transport mechanism of the Ca-ATPase.

ACKNOWLEDGMENT

We thank Diana J. Bigelow for insightful discussions. We also thank Todd D. Williams and Homigol Biesiada of the KU Mass Spectrometry Laboratory for their efforts in acquiring the FAB and electrospray mass spectra.

REFERENCES

1. Inesi, G. (1985) *Annu. Rev. Physiol. 47*, 573−601.
2. Inesi, G. (1994) *Biophys. J. 66*, 554−560.
3. Watanabe, T., and Inesi, G. (1982) *J. Biol. Chem. 257*, 11510−11516.
4. Suzuki, H., Kubota, T., Kubo, K., and Kanazawa, T. (1990) *Biochemistry 29*, 7040−7045.
5. Hansen, O., and Jensen, J. (1995) *Cell Calcium 18*, 557−568.
6. Bishop, J. E., Al-Shawi, M. K., and Inesi, G. (1987) *J. Biol. Chem. 262*, 4658−4663.
7. Inesi, G., Goodman, J. J., and Watanabe, S. (1967) *J. Biol. Chem. 242*, 4637−4643.
8. Verjovski-Almeida, S., and Inesi, G. (1979) *J. Biol. Chem. 254*, 18−21.
9. Barrabin, H., Scofano, H. M., and Inesi, G. (1984) *Biochemistry 23*, 1542−1548.
10. Teruel, J. A., and Inesi, G. (1988) *Biochemistry 27*, 5885−5890.
11. Froehlich, J. P., and Taylor, E. W. (1975) *J. Biol. Chem. 250*, 2013−2021.
12. McIntosh, D. B., and Boyer, P. (1983) *Biochemistry 22*, 2867−2875.
13. Mahaney, J. E., Froechlich, J. P., and Thomas, D. D. (1995) *Biochemistry 34*, 4864−4879.
14. Mignaco, J. A., Lupi, O. T., Santos, F. T., Barrabin, H., and Scofano, H. M. (1996) *Biochemistry 35*, 3886−3891.
15. Fernandez, J. L., Rosemblatt, M., and Hidalgo, C. (1980) *Biochim. Biophys. Acta 599*, 552−568.
16. Lanzetta, P. A., Alverez, L. J., Reinsch, P. S., and Candia, O. (1979) *Anal. Biochem. 100*, 95−97.
17. Warren, G. B., Toon, P. A., Birdsall, N. J. M., Lee, A. G., and Metcalfe, J. (1974) *Proc. Natl. Acad. Sci. U.S.A. 71*, 622−626.
18. Inesi, G., Kurzmack, M., and Lewis, D. (1988) *Methods Enzymol. 157*, 154−190.
19. Lund, S., and Møller, J. V. (1988) *J. Biol. Chem. 263*, 1654−1664.
20. Kanazawa, T., Yamada, S., Yamamoto, T., and Tonomura, Y. (1971) *J. Biochem. (Tokyo) 70*, 95−123.
21. Mitchinson, C., Wildenspan, A. F., Trinnaman, B. J., and Green, N. M. (1982) *FEBS Lett. 146*, 87−92.
22. Birmachu, W., and Thomas, D. D. (1990) *Biochemistry 29*, 3904−3914.
23. Gornall, A., Bardawill, C., and David, M. (1949) *J. Biol. Chem. 177*, 751−766.
24. Shägger, H., and von Jagow, G. (1987) *Anal. Biochem. 166*, 368−379.
25. Wawrzynow, A., and Collins, J. H. (1993) *Biochim. Biophys. Acta 1203*, 60−70.
26. Brandl, C. J., Green, N. M., Korczak, B., and MacLennan, D. H. (1986) *Cell 44*, 597−607.
27. Yao, Y., Yin, D., Jas, G. S., Kuczera, K., Williams, T. D., Schöneich, C., and Squier, T. C. (1996) *Biochemistry 35*, 2767−2787.
28. Yao, Y., Schöneich, Ch., and Squier, T. C. (1994) *Biochemistry 33*, 7797−7810.
29. Morris, S. I., Silbergeld, E. K., Brown, R. R., and Haynes, D. H. (1982) *Biochem. Biophys. Res. Commun. 104*, 1306−1311.
30. Bigelow, D. J., and Inesi, G. (1992) *Biochim. Biophys. Acta 1113*, 323−338.
31. Papp, S., Pikula, S., and Martonosi, A. (1987) *Biophys. J. 51*, 205−220.
32. Froehlich, J. P., and Taylor, E. W. (1976) *J. Biol. Chem. 251*, 2307−2315.
33. Nakamura, S., Suzuki, H., and Kanazawa, T. (1997) *J. Biol. Chem. 272*, 6232−6237.
34. Neet, K. E., and Green, N. M. (1977) *Arch. Biochem. Biophys. 178*, 588−597.
35. Taylor, J. S., and Hattan, D. (1979) *J. Biol. Chem. 254*, 4402−4407.
36. Kosk-Kosicka, D., Kurzmack, M., and Inesi, G. (1983) *Biochemistry 22*, 2559−2567.
37. Vilsen, B., and Andersen, J. P. (1987) *Eur. J. Biochem. 170*, 421−429.
38. de Foresta, B., Le Maire, M., Orlowski, S., Champeil, P., Lund, S., Møller, J. V., Michelangeli, F. M., and Lee, A. G. (1989) *Biochemistry 28*, 2558−2567.
39. Andersen, J. P., Vilsen, B., Nielson, H., and Møller, J. V. (1986) *Biochemistry 25*, 6439−6447.
40. Highsmith, S., and Cohen, J. A. (1987) *Biochemistry 26*, 154−161.
41. Wawrzynow, A., Collins, J. H., and Coan, C. (1993) *Biochemistry 32*, 10803−10811.
42. Bigelow, D. J., and Thomas, D. D. (1987) *J. Biol. Chem. 262*, 13449−13456.
43. Bishop, J. E., Johnson, J. D., and Berman, M. C. (1984) *J. Biol. Chem. 259*, 15163−15171.
44. Inesi, G., Cantilina, T., Yu, X., Nikic, D., Sagara, Y., and Kirtley, M. E. (1992) *Ann. N. Y. Acad. Sci. 671*, 32−48.
45. Dupont, Y., Pougeois, R., Ronjat, M., and Verjovski-Almeida, S. (1985) *J. Biol. Chem. 260*, 7241−7249.
46. Dupont, Y., Chapron, Y., and Pougeois, R. (1982) *Biochem. Biophys. Res. Commun. 106*, 1272−1279.
47. Lacapère, J.-J., Garin, J. Trinnaman, B., and Green, N. M. (1993) *Biochemistry 32*, 3414−3421.
48. Green, M. N. (1989) *Biochem. Soc. Trans. 17*, 970−972.
49. Yamamoto, T., Tagaya, M., Fukui, T., and Kawakita, M. (1988) *J. Biochem. 103*, 452−457.
50. McIntosh, D. B., Wooley, D. G., and Berman, M. C. (1992) *J. Biol. Chem. 267*, 5301−5309.
51. Moutin, M.-J., Cuillel, M., Rapin, C., Miras, R., Anger, M., Lompré, A.-M., and Dupont, Y. (1994) *J. Biol. Chem. 269*, 11147−11154.
52. Taylor, W. R., and Green, N. M. (1989) *Eur. J. Biochem. 179*, 241−248.
53. Stefanova, H. I., Mata, A. M., Gore, M. G., East, J. M., and Lee, A. G. (1993) *Biochemistry 32*, 6095−6103.
54. Bigelow, D. J., and Inesi, G. (1991) *Biochemistry 30*, 2113-2125.
55. Bevington, P. R. (1969) *Data Reduction and Error Analysis for the Physical Sciences*, pp 56−64, McGraw-Hill, New York.

BI980275F